RSC Advances

ROYAL SOCIETY OF CHEMISTRY

www.rsc.org/advances

Graphical and textual abstract

This paper describes the fast stamping of microfluidic paper-based analytical devices with chemically modified surface for improved colorimetric measurements.

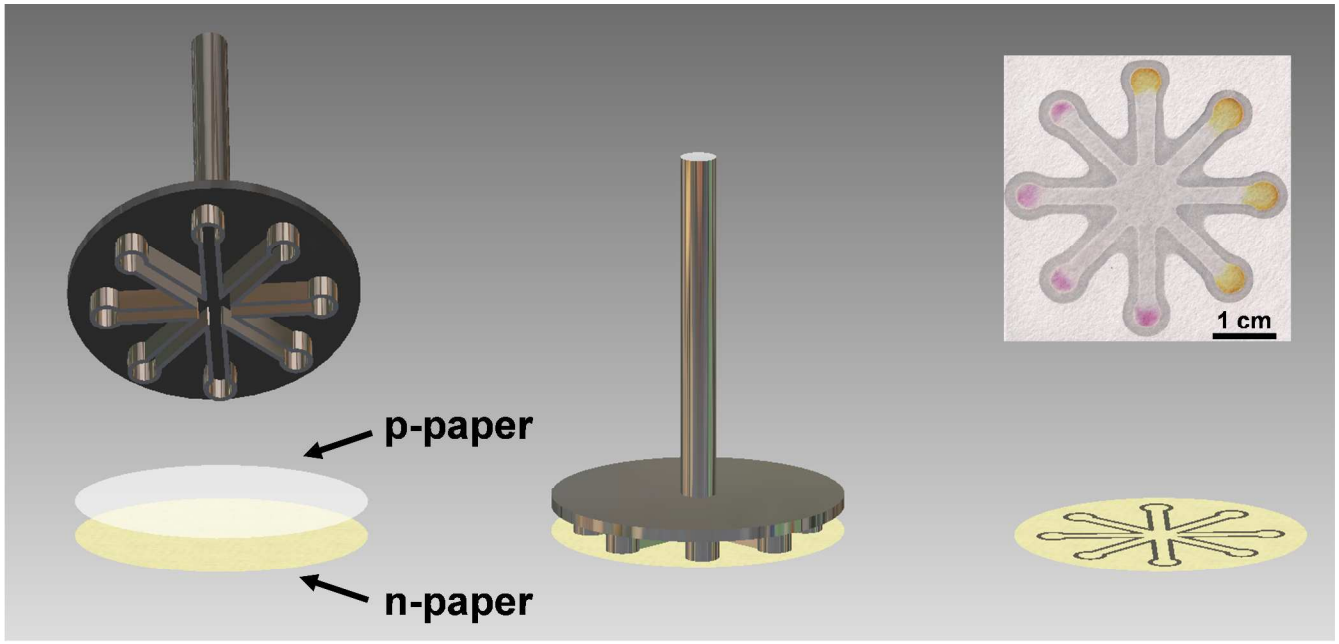

Cite this: DOI: 10.1039/c0xx00000x

www.rsc.org/xxxxxx

ARTICLE TYPE

A handheld stamping process to fabricate microfluidic paper-based analytical devices with chemically modified surface for clinical assays†

Paulo de Tarso Garcia,[a] Thiago Miguel Garcia Cardoso,[a] Carlos Diego Garcia,[b] Emanuel Carrilho[c,d] and Wendell Karlos Tomazelli Coltro*[a,d]

Received (in XXX, XXX) Xth XXXXXXXXX 20XX, Accepted Xth XXXXXXXXX 20XX
DOI: 10.1039/b000000x

This paper describes the development and use of a handheld and lightweight stamp for the production of microfluidic paper-based analytical devices (μPADs). We also chemically modified the paper surface for improved colorimetric measurements. The design of the microfluidic structure has been patterned in a stamp, machined in stainless steel. Prior to stamping, the paper surface was oxidized to promote the conversion of hydroxyl into aldehyde groups, which were then chemically activated for covalent coupling of enzymes. Then, a filter paper sheet was impregnated in paraffin and sandwiched with a native paper (n-paper) sheet, previously oxidized. The metal stamp was preheated at 150 ºC and then brought in contact with the paraffined paper (p-paper) to enable the thermal transfer of the paraffin to the n-paper, thus forming the hydrophobic barriers under the application of a pressure of *ca.* 0.1 MPa during 2 s. The channel and barrier widths measured in 50 independent μPADs exhibited values of 2.6 ± 0.1 and 1.4 ± 0.1 mm, respectively. The chemical modification for covalent coupling of enzymes on the paper surface also led to improvements on the colour uniformity generated inside the sensing area, a known bottleneck in this technology. The relative standard deviation (RSD) values for glucose and uric acid (UA) assays decreased from 40 to 10% and from 20 to 8%, respectively. Bioassays related to the detection of glucose, UA, bovine serum albumin (BSA), and nitrite were successfully performed in concentration ranges useful for clinical assays. The semi-quantitative analysis of all four analytes in artificial urine samples revealed an error smaller than 4%. The disposability of μPADs, the low instrumental requirements of the stamp-based fabrication, and the improved colour uniformity enable the use of the proposed devices for the point-of-care diagnostics or in limited resources settlements.

Introduction

Microfluidic paper-based analytical devices (μPADs) have recently demonstrated high potential to be applied in a variety of bioanalytical studies involving sensing and diagnostic applications.[1-6] This low cost platform was proposed for microfluidic applications in 2007 by the Whitesides group.[4] Since then, μPADs have received growing attention due to the global affordability of paper substrates as well as great advantages for the point-of-care testing (POCT), which include disposability, portability, biocompatibility, and capability of performing assays without traditional instrumentation[1,3,6-8] The fabrication of the microfluidic network in paper substrates usually requires the creation of hydrophobic barriers to define the region where the fluid flows. Due to the hydrophilic nature of paper, the lateral flow action induces the fluidic transport through the porous structure of the substrate.[9,10] Hydrophobic barriers have been often formed by different techniques including photolithography,[4,11] wax printing,[12,13] screen-printing,[14] flexography,[15] laser treatment[16] as well as plotting of poly(dimethylsiloxane) (PDMS)[17] or permanent (indelible) markers (ink).[18] Other approaches including the use of inkjet etching,[19] laser cutting,[20,21] and wax dipping[22] for the fabrication of μPADs have also been reported.

The application of μPADs in clinical assays has been reported in association with different detection systems including colorimetric,[23,24] electrochemical,[25-29] chemiluminescence[30,31] and mass spectrometry[32,33]. Image-based analysis has been one of the most popular detection systems used by most the researchers due to its instrumental advantages (portability and capacity of performing analysis via telemedicine with cell-phone cameras[21]).

[a] *Instituto de Química, Universidade Federal de Goiás,74001-970, Goiânia, GO, Brazil*
[b] *Department of Chemistry, The University of Texas at San Antonio, One UTSA Circle, San Antonio, TX, USA*
[c] *Instituto de Química de São Carlos, Universidade de São Paulo, 13566-970, São Carlos, SP, Brazil*
[d] *Instituto Nacional de Ciência e Tecnologia de Bioanalítica, 13084-971, Campinas, SP, Brazil*
**E-mail: wendell@ufg.br*
†Electronic Supplementary Information (ESI) available. See DOI: 10.1039/b000000x/

In all cases, the use of colorimetric measurements requires the incorporation of coloured (or chromogenic) reagents on the surface of the μPADs to reveal the presence of the target analytes and consequently induce the changes in the colour in the detection zones. As recently reported by Yetisen and co-workers,[34] however, the performance of most colour-based enzymatic assays on μPADs is negatively affected by the non-uniformity of the resulting signal in the sensing areas.[34,35] This problem generates uncertainty and the result could be influenced by the selection of the area used to analyze the pixel histogram. Recently, Evans and co-workers demonstrated that the rational selection of paper substrates based on their porosity or thickness can be a simple strategy to overcome the problems associated with the lack of colour uniformity on colorimetric measurements.[35] Besides the substrate type, the chemistry involved in the paper composition is well known and it reveals an opened venue to be investigated for sensing applications on μPADs in association with digital-image analysis.[31,36,37]

Considering the advantages and the current limitations of μPADs, this manuscript presents a handheld and lightweight stamp that produces μPADs in matter of seconds as well as reports a strategy to chemically modify the paper surface and improve the colour uniformity of the detection zones. For the fabrication of the stamp, the layout of the microfluidic structure was machined on a metal surface and then used for the rapid prototyping of μPADs. The stamp was pre-heated and placed in contact with a previously paraffined paper (p-paper). The direct contact allowed the transference of an amount of paraffin to a native paper (n-paper) located below the paraffined piece, thus creating hydrophobic barriers with great reproducibility by a single stamping stage.

Although a recent paper has reported improvements on the colour intensity and uniformity based on the paper properties, we propose the chemical immobilization of glucose oxidase and uricase enzymes on sensing zones to ensure their binding on the cellulose fibers. To demonstrate this proof-of-concept, the surface of the paper was first oxidized to convert the hydroxyl into aldehyde groups. Prior to colorimetric assays, the aldehyde groups were chemically activated for covalent coupling of glucose oxidase and uricase enzymes involved in the glucose and uric acid (UA) assays. In addition to glucose and UA assays, complexometric assays for bovine serum albumin (BSA) and nitrite have also been successfully performed. The clinical feasibility of the stamped μPADs was demonstrated with the detection of four compounds in biological samples.

Material and methods

Materials and chemicals

Potassium iodide, D-trehalose dihydrate, glucose oxidase (181 U/mg), horseradish peroxidase (73 U/mg), D-glucose, sodium citrate, chloride acid, ethanol, sodium monohydrogen phosphate, sodium dihydrogen phosphate, tetrabromophenol blue (TBPB), bovine serum albumin (BSA), citric acid, sulfanilamide, N-(1-napthyl) ethylenediamine, sodium nitrite, uric acid (UA), uricase (from *Candida sp.*, 2 U/mg), 4-aminoantipyrine (AAP), 3,5-dichloro-2-hydroxy-benzenesulfonic acid (DHBS), sodium periodate, N-(3-Dimethylaminopropyl)-N′-ethylcarbodiimide hydrochloride (EDC) and N-hydroxysuccinimide (NHS) were acquired from Sigma Aldrich Co. (Saint Louis, MO, USA). Filter paper (model JP 40, 12.5 cm diameter and 25 μm porous) was purchased from JProlab (São José dos Pinhais, PR, Brazil). Paraffin (code 140º/145ºF) was acquired from Petrobras (Rio de Janeiro, RJ, Brazil). A multifunctional DeskJet printer (model F4280) was purchased from Hewlett-Packard (Palo Alto, CA, USA) to perform colorimetric measurements through the scanner mode. Scanning Electron Microscopy (SEM) was performed using a JEOL microscope (model JSM-6610, Waltham, MA, USA). For SEM analyses, a square paper piece (10 x 10 mm) was used. All reagents were analytical grade and used as received.

Fabrication of μPADs

The fabrication of μPADs was carried out as schematically described in Figure 1. Initially, a filter paper sheet was immersed into liquid paraffin (at 90º C) during 60 seconds. The paper was then removed from the paraffin, allowed to solidify at room temperature and then placed on the n-paper surface. A metal stamp, machined in stainless steel by a local shop (MS Máquinas, Goiânia, GO, Brazil), was preheated at 150 ºC in a hot plate for 2 minutes and brought in contact with the p-paper to stamp the microfluidic structure on the n-paper. The application of a pressure of *ca.* 0.1 MPa during 2 s to the stamp enabled the thermal transfer of the paraffin from the p-paper to the n-paper, thus forming the hydrophobic barriers. μPADs were designed in a geometry containing eight circular detection zones for bioassays interconnected by microfluidic channels and one central zone to sample inlet. All channels were nominally fabricated with a 10-mm length and 3-mm width. The diameter values for detection and central zones were 5 and 10 mm, respectively. The final dimensions of μPADs were 45 mm × 45 mm.

Colorimetric detection

Colorimetric detection was performed with the scanner mode of a DeskJet multifunction printer (Hewlett-Packard, model F4280) using a 600-dpi resolution. The recorded images were first converted to a 24-bits colour scale (RGB dimension) and then analyzed in Corel Photo-Paint™ software. The arithmetic mean of the pixel intensity within each test zone was used to quantify the colour intensity.

Bioassays

The detection zones for nitrite assays were sequentially spotted with 0.75 μL aliquot of colour solution containing of mixture 50 mmol L^{-1} sulfanilamide, 330 mmol L^{-1} citric acid and 10 mmol L^{-1} N-(1-napthyl)ethylenediamine, previously prepared in methanol. After each addition, the zones were allowed to dry at room temperature during 10 min. For BSA assays, the detection zones were first spotted with 0.75 μL of 250 mmol L^{-1} citric acid and then 0.75 μL of 3 mmol L^{-1} TBPB. After each addition, the zones were also allowed to dry at room temperature during 10 min. The detection zones for glucose assays were prepared according to a procedure described by Martinez and co-workers.[23] First, a 0.75-μL aliquot of a solution containing 0.6 mol L^{-1} potassium iodide and 0.3 mol L^{-1} trehalose was added on all detection zones and dried at room temperature.

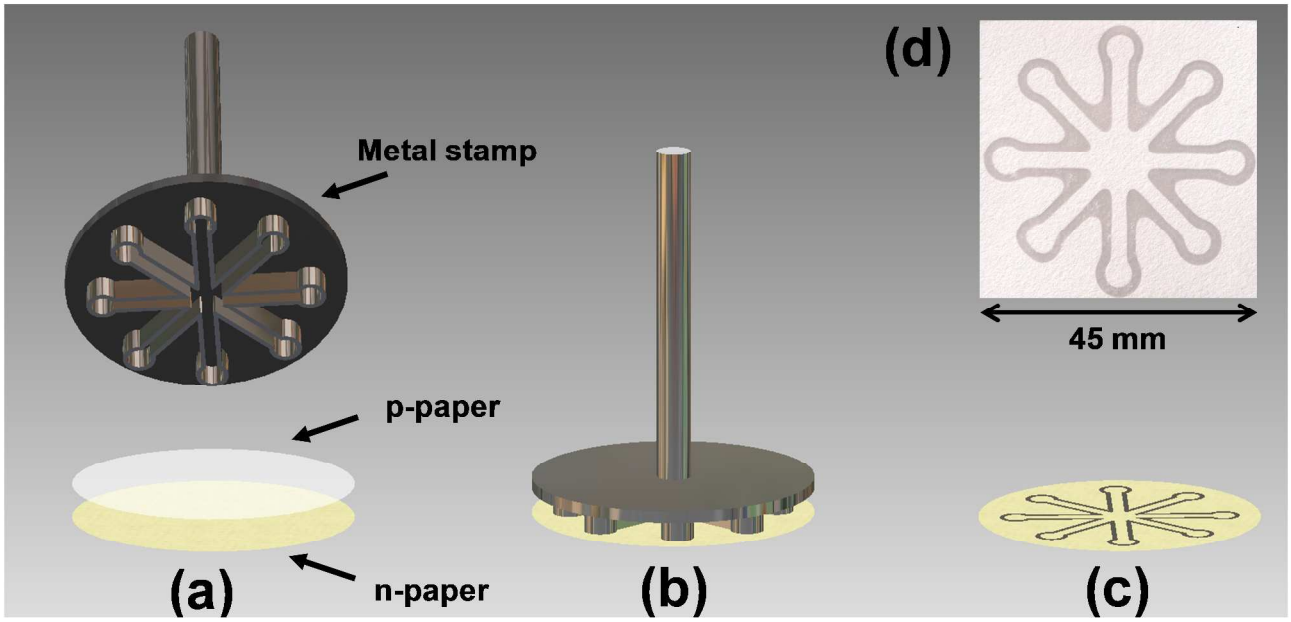

Fig. 1 Scheme of the fabrication process of µPADs based on stamping. In (a), a paraffinized paper (p-paper) is placed over the native paper (n-paper) surface; In (b), the metal stamp is heated at 150 °C and brought into contact with the layered paper pieces; Step (c) represents a typical µPAD fabricated by the proposed method. The optical micrograph in (d) depicts a real image showing the stamped µPAD.

Then, 0.75 µL aliquots of a solution containing glucose oxidase and horseradish peroxidase (5:1) prepared in 100 mmol L^{-1} phosphate buffer (pH 6.0) were added on all zones and allowed to dry at room temperature during 10 min. For UA assays, the detection zones were prepared according to a procedure described by Dungchai and co-workers.[24] Initially, all detection zones were spotted with 0.75 µL aliquots of colour reagent consisted of a mixture of 4 mmol L^{-1} AAP and 8 mmol L^{-1} DHBS. Afterwards, 0.75 µL aliquots of a solution containing uricase (80 U/mL) and horseradish peroxidase (339 U/mL) were added on all detection zones and allowed to dry at room temperature during 10 min. All assays were performed by adding 40 µL of standard or artificial sample solutions to the central zone which promoted the quick and even distribution of the sample through microfluidic channels by capillary action towards the detection zones.

Chemical modification of the paper surface

Paper substrates were chemically modified to allow the covalent coupling of enzymes on the cellulose surface. Prior to stamping, the paper sheets were immersed in a petri dish containing 10 mL of 0.5 mol L^{-1} $NaIO_4$ solution and allowed to react at room temperature and in the dark for 30 min, to produce aldehyde groups. After oxidation, the paper sheets were washed three times with ultrapure water. µPADs were then stamped according to procedure described earlier. All detection zones for enzymatic assays were spotted with a mixed solution of EDC (0.1 mol L^{-1}) and NHS (0.1 mol L^{-1}) in ultrapure water. Aliquots of 0.75 µL were added in each zone and allowed to dry at room temperature during 20 min to convert the aldehyde groups of the cellulose to amine reactive esters. Afterwards, enzymes were covalently conjugated on the modified-paper surface by adding of 0.75 µL of enzyme solution on the detection zones.

Artificial Urine Sample

The clinical feasibility of the stamped µPADs was investigated with urinalysis tests for four bioassays. For this purpose, an artificial urine solution was prepared according to the procedure previously reported by Brooks and Keevil.[38] The stock solutions of nitrite, BSA, glucose, and UA were prepared and diluted using the artificial urine. The final concentrations for nitrite, BSA, glucose and UA were 100 µmol L^{-1}, 35 µmol L^{-1}, 4 mmol L^{-1}, and 3 mmol L^{-1}, respectively.

Results and discussion

Choice of paraffin

Paraffin was chosen for the fabrication of hydrophobic barriers due to its thermoplastic properties, low melting temperature (60 ± 2 °C) and low cost (*ca.* $1.00 per kilogram). Furthermore, it is a white soft solid with resistance to most chemical compounds used in the proposed assays.[39] Besides these advantages, paraffin is the major component of solid ink[40] and has been extensively used in the fabrication of µPADs by wax printing technology.[12,13] The use of paraffin to create hydrophobic barriers in paper was independently described by Yagoda[39] and Müller and Clegg[41] in the past century. In these two pioneer papers, the authors reported the fabrication of printed zones in paper as well as a restricted area for demonstrating the elution of a mixture of pigments. In the study reported by Müller and Clegg,[41] a heat press was used to provide the impregnation of paraffin on a filter paper surface. However, the delimited area depends on the wire ductility to configure complex geometries. In 2012, Zhang and Zha[42] used paraffin to produce hydrophobic walls in paper surfaces. Basically, the authors patterned the microfluidic structure in a copper sheet by a sequence of thermal transfer and wet chemical etching steps. The copper surface was covered with solid paraffin

to allow the thermal transference to the paper surface with an electric iron. This process is laborious and requires *ca.* 1.5 h to obtain paper-based devices.

Stamping-based fabrication

More recently, the development of stamping-based methods[18,43] for producing μPADs has been reported as alternative fabrication protocols in comparison to conventional techniques. Curto *et al.*[18] developed a PDMS high-relief stamp based on a template previously defined in PMMA. The features defined in PDMS were used for replicate microfluidic structures in chromatographic paper by stamping of indelible ink within 10 s. Zhang *et al.*[43] reported the fabrication of a iron stamp based on the principle of movable-type printing. This equipment-free tool allows the assembling of a desirable arrangement with adjustable magnetic field. The authors successfully described the production of paper microplates and μPADs with different geometries based on the transference of wax to the paper surface. In both reports, the stamps presented a weight of *ca.* 500 g. Here, we present the results collected with μPADs fabricated using a handheld, low-cost, and lightweight stamp. The process can be completed in less than 5 s and is based on the creation of paraffin barriers. The stamp was machined using stainless steel in less than 4h at a local shop. In comparison to other stamps recently reported, the proposed stamp offers instrumental simplicity, portability and low cost (*ca.* $50). Furthermore, it is lightweight (*ca.* 80 g), durable, and resistant to the air oxidation. Even with a cost estimated in *ca.* $50, we have fabricated more than 5,000 μPADs with the same stamp. This feature could allow the fabrication of devices in places with limited resources or where the access to standard fabrication technologies is restricted.

Characterization

The creation of paraffin barriers is simple and it can be completed within seconds. Briefly, when the heated stamp is placed in contact with the upper paper piece (p-paper), the paraffin melts and penetrates through the porous structure towards the bottom paper piece (n-paper). During this process, hydrophobic barriers were defined just in regions where the stamp had contact with the paper surface. This process has allowed producing effective hydrophobic barriers where sample leaking was not observed in either the front or the back side of the paper (see Figures S-1 and S-2, available in ESI). To test for leaks, a solution containing small amounts of surfactants (such as Triton X-100, 0.5 % v/v) was used. As this solution has lower surface tension, it quickly wicks the paper, revealing incomplete paraffin barriers. This procedure was also recently used by Rosa and co-workers.[44] When compared to other fabrication techniques, the time required for stamping-based prototyping of μPADs has the potential to be significantly shorter. To optimize the transfer time, we have investigated the transference of paraffin barriers in a time ranging from 1 to 10 s. Taking into account that the proposed technique is based on the paraffin melting, the stamping time at constant pressure promotes the transference of different amounts of paraffin to the n-paper surface. As it can be seen in Figure S-3A (available in ESI), the amount of paraffin transferred from p-paper to n-paper increases from 15 to 35 mg per device when the time rises from 1 and 10 s. However, stamping times longer than 5 s should be avoided, as the channel could be partial or totally blocked due to the excess of paraffin. In addition, it is important to note that the mass transferred under stamping times longer than 6 s is quite similar. This behaviour may be attributed to the thickness of the stamp edges, which limits the amount of paraffin transferred from the p-paper to the n-paper. Figure 2 shows three representative optical micrographies of μPADs stamped during 2, 5 and 10 s.

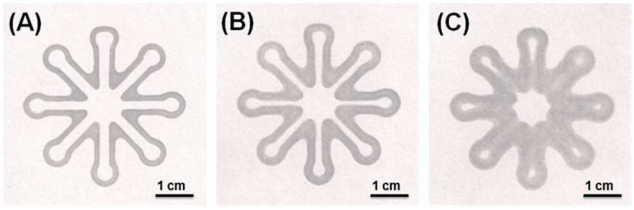

Fig. 2 Optical micrographs showing examples of μPADs stamped during (A) 2, (B) 5 and (C) 10 seconds.

In addition to the amount of paraffin, the channel and the paraffin barrier widths are also dependent on the stamping time. The channel and barrier widths ranged, respectively, from 2.5 to 2.0 mm and from 1.4 to 2.2 mm when the stamping time increased from 2 to 5 s. On the other hand, the channel was completely blocked after stamping of 10 s. Based on the optical images shown in Figure 2, it can be inferred that the paraffin melts and penetrates the porous structure in both vertical and horizontal orientations. This phenomenon justifies the observed changes in terms of width for the channel and also the hydrophobic barrier. For this reason, the stamping of μPADs has been kept at 2 s. The handheld tool proposed to easily replicate μPADs does not compromise the device-to-device reproducibility. As it can be seen in Figure S-3B, the widths for 50 similar μPADs have exhibited an average value of 2.6±0.1 mm. For each device, the width was measured at three different points with a relative standard deviation (RSD) ranging from 1 to 7%. It is important to highlight that the stamping of μPADs was manually performed under the application of *ca.* 2 kg onto the metal stamp. Once the superficial area is known, the pressure was estimated to be *ca.* 0.1 MPa.

The morphology of the paper substrates has been studied by SEM analysis for a better understanding on the creation of paraffin barriers. Figures 3A and 3B show SEM images for the paper surface before and after the stamping of paraffin on n-paper, respectively. Based on these images, it possible to observe that the porous structure of the paper substrate is completely filled with paraffin after the stamping stage, thus creating the hydrophobic barrier required for microfluidic applications. Figure 3C displays SEM image from the sectional view of a paper-based channel defined with paraffin. As mentioned earlier, the paraffin vertically penetrates through the cellulose porous defining the hydrophobic barrier after solidification step. Likewise the channel width, the reproducibility for the hydrophobic barrier width was also investigated keeping the stamping time in 2 s. The barrier width measured in 50 independent channels presented a value of 1.4 ± 0.1 mm.

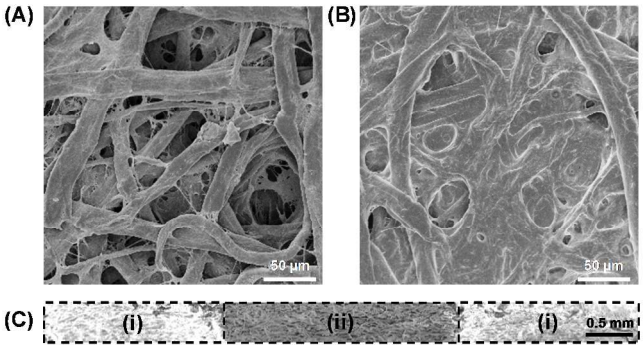

Fig. 3 SEM images showing the morphology of the paper surface (A) before and (B) after deposition of paraffin barriers by stamping, as well as a cross-sectional view of the resulting microfluidic channel structure. In (C), the labels (i) and (ii) mean the paraffin barriers and the channel, respectively.

Bioassays

The feasibility of the stamped µPADs was demonstrated with colorimetric sensing of nitrite, BSA, glucose and UA. Initially we tested a µPAD prepared on n-paper substrate (without chemical modification) to perform all simultaneously complexometric (zones labelled from 1 to 4) and enzymatic (zones labelled from 5 to 8) assays. As depicted in Figure 4, it can be observed that the colour intensity for the enzymatic assays (glucose and UA) did not exhibit homogeneity into detection zones. This effect was recently mentioned in a review article[34] and was directly related to the surface chemistry of the paper. When the enzyme is added on the n-paper, it adsorbs on the porous structure due to the electrostatic interactions. In this case, the lack of a strong and effective bond between the enzyme and the paper surface allows carrying the enzymes towards the edges of the sensing zone when the bioassay is performed under lateral flow. Consequently, a gradient of colour (ranging from colorless to brown for the glucose assay) is typically generated in the detection zones. Similar effects were also observed in detection zones for UA. The RSD values associated with the colour gradient observed for glucose and UA assays were *ca.* 40 and 20%, respectively. These values were directly provided by the software histogram as function of the standard deviation for the mean pixel intensity measured on each zone.

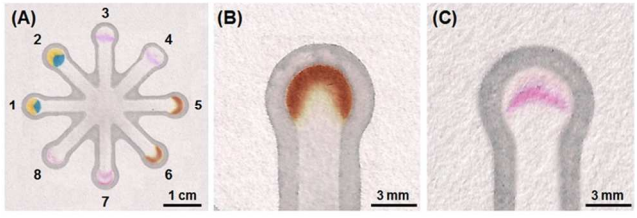

Fig. 4 Optical micrographies of the stamped µPAD for multi-analyte testing showing: (A) simultaneous assays for BSA (zones labelled 1-2), nitrite (zones 3-4), glucose (zones 5-6), and UA (zones 7-8); and an illustration of the common problems associated with the colour gradient generated for (B) glucose and (C) UA being washed towards the edge of the zone, impairing an optical detection based on the counting of pixels inside the zone.

In order to improve the colour gradient highlighted in Figs. 4B and 4C, paper substrates were oxidized with sodium periodate prior to the stamping stage in order to convert the hydroxyl to aldehyde groups. This chemical modification of the paper surface was verified by infrared spectroscopic analysis, in which a characteristic peak of aldehyde groups was observed only on the oxidized paper at 1727 cm^{-1}, as shown in Figure S-4 (available in ESI). The aldehyde groups on the oxidized paper surface were then activated with a solution containing EDC-NHS enabling the covalent coupling of enzyme on the substrate. This procedure has been employed to provide the immobilization of biomolecules on paper or threads.[31, 45] The chemical modification has positively improved the colour uniformity for enzymatic assays. On the other hand, the use of oxidized paper has not provided improvements in the colour uniformity for complexometric assays, as depicted in Figure S-5 (available in ESI). In addition, interferences were observed in the detection zones for nitrite on oxidized µPADs, which may be regarded to a possible reaction between sulfanilamide and the oxidized paper. For this reason, we have decided to use native µPADs for complexometric assays and oxidized µPADs for enzymatic tests.

Figure 5 shows optical micrographs for the glucose and UA assays carried out on oxidized µPADs. As denoted in Figure 5, the colour intensity has demonstrated better uniformity when compared to the assays on native substrates (Fig. 4). The RSD values achieved for the colour gradient related to the glucose and UA were *ca.* 10 and 8%, respectively. In comparison with the results for the native µPADs, the chemical modification has ensured a much better colour uniformity. This improvement solves the problem commonly addressed to the colorimetric measurements and also offers higher reliability for the user analyzing the colour intensity.

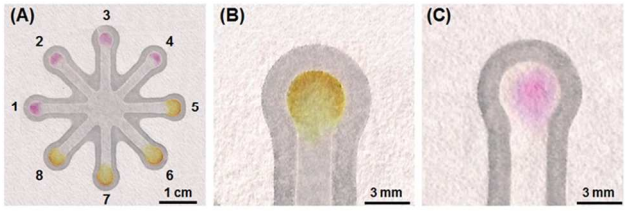

Fig. 5 Optical micrographs of previously oxidized stamped µPAD for multi-analyte testing showing: (A) simultaneous enzymatic assays for UA (zones 1-4) and glucose (zones 5-8) and the details for colour gradient for (B) glucose and (C) UA on µPADs produced with chemically modified surface.

Analytical performance

The analytical performance of the treated stamped µPADs was investigated in order to evaluate their feasibility for quantitative determination in clinical samples. According to the analytical curves presented in Figure 6, the assays for nitrite, glucose, and UA have exhibited good linearity for the concentration ranges from 0−150 µmol L^{-1}, 0−12 mmol L^{-1} and 0−5 mmol L^{-1}, respectively. For these three assays, the correlation coefficient values were greater than 0.993. On the other hand, the BSA assay has displayed a non-linear profile for a concentration range between 0−60 µM.

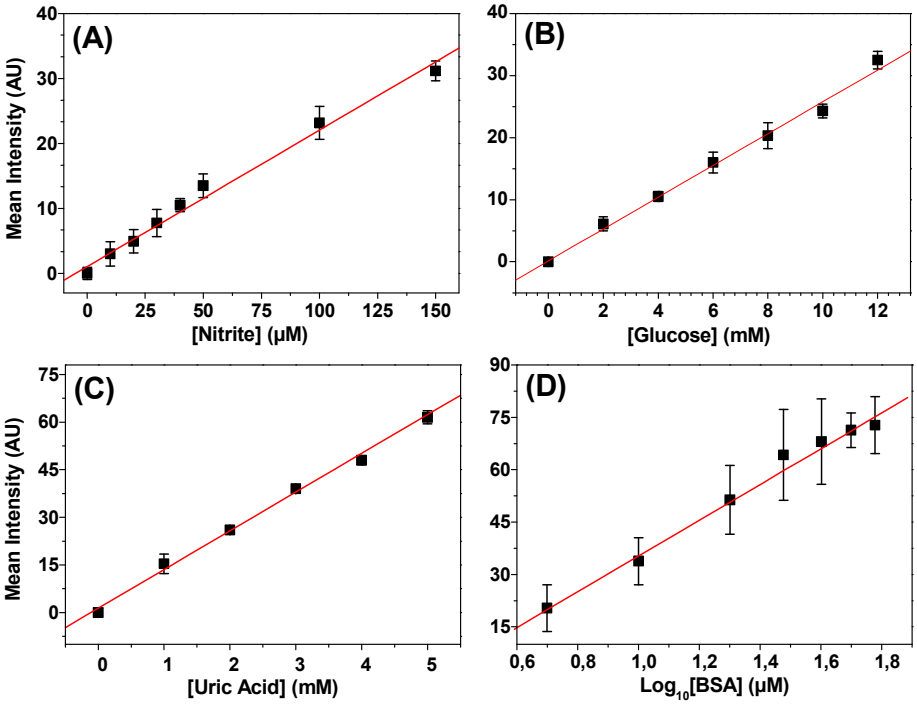

Fig. 6 Analytical curves for (A) Nitrite, (B) glucose, (C) uric acid and (D) BSA. The respective equations were: $y_{Nitrite}$= 1.024 + 0.210· [Nitrite]; $y_{Glucose}$= 2.970 + 2.322· [Glucose], $y_{UricAcid}$= 0.260 + 12.920· [Uric Acid] and y_{BSA}= -15.898 + 51.180· Log_{10}[BSA].

The data were then linearized to show a linear relationship between the mean intensity and the logarithm of the concentration of BSA with a correlation coefficient of 0.997.

The limit of detection (LOD) for each bioassay was calculated based on the relation between three times the standard deviation for the blank (SD) and the angular coefficient (*b*) of the respective analytical curve (LOD = (3·SD)/*b*). The LOD values achieved for nitrite, glucose, UA, and BSA were 13.2 μmol L^{-1}, 0.7 mmol L^{-1}, 0.3 mmol L^{-1}, and 3.1 μmol L^{-1}, respectively. These values are similar to those previously reported.[23,36,46-48] It is important, however, to highlight that the chemical modification on the paper surface affects the sensitivity of the colorimetric measurements. As displayed in Figure S-6, the slope of the curves associated with native (b = 10.6 AU/mmol L^{-1}) and oxidized (b = 2.6 AU/mmol L^{-1}) paper are quite different. This is related to the colour uniformity inside the detection zones and the preconcentration effect that occurs in the presence of the lateral flow for assays on native paper. Since the enzyme is not covalently bound on the paper surface, it is washed out to the edges generating higher intensities at the edge than the zone centre. Consequently, the LOD value is directly influenced for this effect. Based on the data available in Figure S-6, the LOD values for the glucose assay performed on native and oxidized μPADs were 0.1 and 0.7 mmol L^{-1}, respectively. Likewise the improvements observed for the colour uniformity, the use of oxidized paper has also led to better precision for eight independent measurements on μPADs. The RSD values found for six glucose concentration levels ranged from 4 to 8%. Despite the lower sensitivity achieved on oxidized μPADs, the analytical performance has been suitable for applications in the clinical ranges.

The choice of glucose, BSA, UA, and nitrite is regarded to theirclinical importance in the urinalysis. The normal levels of glucose and UA in urine are 0.1–0.8 mmol L^{-1}, and 1.5–4.4 mmol L^{-1}, respectively. Glucose concentrations above the normal range may be indicative of diabetes or renal glycosuria.[49] Likewise glucose, UA concentrations higher than normal range may represent a diagnostic of gout, rheumatology, or hyperuricemia.[50] The presence of albumin in urine can be helpful to distinguish common diseases including proteinuria and nephrotic syndrome.[23] The clinical range comprises concentrations between 0 and 60 μmol L^{-1}. On the other hand, the nitrite assay is commonly performed to diagnostic the urinary tract infection, which occurs due to the presence of bacteria, such as *Escherichia coli*. This bacterium enzymatically converts the nitrate to nitrite. Clinical diagnostics of nitrite are conventionally carried out with dipstick tests, which provide qualitative information for concentrations above 16 μmol L^{-1}.[51] According to the normal ranges presented by medical associations, the analytical parameters found with the stamped μPADs are suitable for clinical purposes, once they can provide helpful information about the concentration levels of the four analytes mentioned.

Despite the LOD obtained for the glucose assay using oxidized paper (0.7 mmol L^{-1}), oxidized μPADs can be used for determination of normal levels of glucose in urine (0.1–0.8 mmol L^{-1}) with the standard addition method. Considering that normal levels of glucose in other biological samples (such as blood) are higher than in urine sample, the proposed method could be extended to other applications. On the other hand, the LOD achieved for the bioassays could be improved based on the rational selection of paper substrates for the fabrication of μPADs. As recently described by Evans and colleagues,[35] the

colour intensity depends on the paper substrate properties like thickness and porosity, for example. This strategy would be interesting for using the stamped μPADs in the entire clinical range.

Quantitative analysis in artificial urine

The concentration levels of glucose, UA, nitrite, and BSA were determined in artificial samples using the proposed stamped μPADs. Basically, one artificial urine sample was prepared containing known concentrations of all four analytes. Enzymatic and complexometric assays were performed on oxidized and native μPADs, respectively. The values found are presented in Table 1. Based on the data shown, we can conclude that the use of μPADs offers good accuracy and precision. The RSD values for eight measurements (four per device) ranged from 0.9 to 4.5% and from 12 to 17% for complexometric and enzymatic assays, respectively. When compared to the known concentrations, the error achieved was smaller than 4%, indicating that the proposed devices have great potential for the quantitative determination in clinical samples.

Table 1 Analytical performance of μPAD assays for the urine analysis with stamped paraffin devices with native and oxidized paper.

Analytes	Known concentration	Found concentration
Nitrite* (μmol L^{-1})	100.0	103 ± 1
BSA* (μmol L^{-1})	35.0	34 ± 2
Glucose** (mmol L^{-1})	4.0	4.1 ± 0.5
Uric Acid** (mmol L^{-1})	3.0	2.9± 0.5

*Assays performed on μPADs fabricated with native paper.
**Assays performed on μPADs fabricated with oxidized paper.

Conclusions

In summary, we reported the development and use of a handheld, portable, and lightweight stamp for rapid prototyping of μPADs made with paraffin over chemically modified paper substrate for clinical assays with image-based detection. The stamp has enabled the creation of paraffin barriers on paper substrates in less than 5 s with minimal instrumental requirements. The choice of paraffin for stamping of μPADs is attractive due to its low cost and lower melting point than wax ink often used in the wax printing method.[13] The time required to obtain the paraffin-impregnated paper piece is lower than 2 minutes. In comparison with most popular fabrication techniques like wax printing, screen-printing, and photolithography, the stamp-based approach offers simplicity, portability, and capability of producing μPADs in matter of seconds. The cost of a stamp machined in stainless steel has been estimated to be *ca.* $50 and it has allowed the fabrication of more than 5,000 μPADs with great reproducibility and no sign of degradability. The final cost of one μPAD defined with paraffin barriers was *ca.* $0.04.

Moreover, this paper also addressed improvements on the colour uniformity inside sensing zones, which has been achieved based on the chemical modification of the paper surface. The oxidation of hydroxyl to aldehydes groups by periodate followed by activation with EDC-NHS allowed the covalent coupling of enzymes (glucose oxidase and uricase) on the cellulose substrate. As a consequence, the colour gradient generated after colorimetric assays presented better uniformity and reproducibility due to the absence of washing-out of the coloured products promoted by the capillary action, when using non-linked enzymes, to the detection zone edges. The RSD values for glucose and UA assays decreased from 40 to 10% and from 20 to 8%, respectively. The enhanced colour uniformity clearly shows that colorimetric analysis can provide quantitative data with great reliability. This clinical feasibility has been successfully demonstrated with the detection of nitrite, BSA, UA, and glucose in artificial urine samples with error between 2.5 and 4.0%.

Finally, we believe that the advantages offered by the fabrication technique proposed herein in association with the improvements achieved with the chemically modified paper surface can stimulate the implementation of low-cost urinalysis in places with limited resources as well as in clinical laboratories where the quantitative analysis with great reliability is required.

Acknowledgments

This project was supported by Conselho Nacional de Desenvolvimento Científico e Tecnológico (CNPq)—grant No. 478911/2012-2, Fundação de Amparo à Pesquisa do Estado de Goiás (FAPEG), and the Instituto Nacional de Ciência e Tecnologia de Bioanalítica (INCTBio). CNPq is also acknowledged for the scholarships granted to PTG and TMGC and research fellowships granted to EC and WKTC (grant Nos. 311323/2011-1 and 311744/2013-3, respectively). The authors would like to thank Professor Charles S. Henry, Ms. Lorrana Nóbrega, and Mr. João Bruno Santos for discussion about the UA assay, drawings in Figure 1 and assistance on the first steps of this study, respectively.

References

1. W. K. T. Coltro, D. P. de Jesus, J. A. F. da Silva, C. L. do Lago and E. Carrilho, *Electrophoresis*, 2010, 31, 2487-2498.
2. J. Hu, S. Wang, L. Wang, F. Li, B. Pingguan-Murphy, T. J. Lu and F. Xu, *Biosensors & bioelectronics*, 2014, 54, 585-597.
3. A. W. Martinez, S. T. Phillips, G. M. Whitesides and E. Carrilho, *Anal. Chem.*, 2010, 82, 3-10.
4. A. W. Martinez, S. T. Phillips, M. J. Butte and G. M. Whitesides, *Angew. Chem. Int. Ed.*, 2007, 46, 1318-1320.
5. X. Li, D. R. Ballerini and W. Shen, *Biomicrofluidics*, 2012, 6, 011301, DOI: 10.1063/1061.3687398.
6. S. Byrnes, G. Thiessen and E. Fu, *Bioanalysis*, 2013, 5, 2821-2836.
7. E. W. Nery and L. T. Kubota, *Anal. Bioanal. Chem.*, 2013, 405, 7573-7595.
8. M. Santhiago, E. W. Nery, G. P. Santos and L. T. Kubota, *Bioanalysis*, 2014, 6, 89-106.
9. E. Fu, B. Lutz, P. Kauffman and P. Yager, *Lab Chip*, 2010, 10, 918-920.

10. J. L. Osborn, B. Lutz, E. Fu, P. Kauffman, D. Y. Stevens and P. Yager, *Lab Chip*, 2010, 10, 2659-2665.
11. A. W. Martinez, S. T. Phillips and G. M. Whitesides, *Proc. Natl. Acad. Sci. U. S. A.*, 2008, 105, 19606-19611.
12. Y. Lu, W. W. Shi, L. Jiang, J. H. Qin and B. C. Lin, *Electrophoresis*, 2009, 30, 1497-1500.
13. E. Carrilho, A. W. Martinez and G. M. Whitesides, *Anal. Chem.*, 2009, 81, 7091-7095.
14. W. Dungchai, O. Chailapakul and C. S. Henry, *Analyst*, 2011, 136, 77-82.
15. J. Olkkonen, K. Lehtinen and T. Erho, *Anal. Chem.*, 2010, 82, 10246-10250.
16. G. Chitnis, Z. W. Ding, C. L. Chang, C. A. Savran and B. Ziaie, *Lab Chip*, 2011, 11, 1161-1165.
17. D. A. Bruzewicz, M. Reches and G. M. Whitesides, *Anal. Chem.*, 2008, 80, 3387-3392.
18. V. F. Curto, N. Lopez-Ruiz, L. F. Capitan-Vallvey, A. J. Palma, F. Benito-Lopez and D. Diamond, *RSC Adv.*, 2013, 3, 18811-18816.
19. K. Abe, K. Suzuki and D. Citterio, *Anal. Chem.*, 2008, 80, 6928-6934.
20. P. Spicar-Mihalic, B. Toley, J. Houghtaling, T. Liang, P. Yager and E. Fu, *J. Micromech. Microeng.*, 2013, 23, 067003, DOI: 10.1088/0960-1317/1023/1086/067003.
21. J. F. Nie, Y. Z. Liang, Y. Zhang, S. W. Le, D. N. Li and S. B. Zhang, *Analyst*, 2013, 138, 671-676.
22. T. Songjaroen, W. Dungchai, O. Chailapakul and W. Laiwattanapaisal, *Talanta*, 2011, 85, 2587-2593.
23. A. W. Martinez, S. T. Phillips, E. Carrilho, S. W. Thomas, H. Sindi and G. M. Whitesides, *Anal. Chem.*, 2008, 80, 3699-3707.
24. W. Dungchai, O. Chailapakul and C. S. Henry, *Anal. Chim. Acta*, 2010, 674, 227-233.
25. W. Dungchai, O. Chailapakul and C. S. Henry, *Anal. Chem.*, 2009, 81, 5821-5826.
26. R. F. Carvalhal, M. S. Kfouri, M. H. D. Piazetta, A. L. Gobbi and L. T. Kubota, *Anal. Chem.*, 2010, 82, 1162-1165.
27. Z. H. Nie, C. A. Nijhuis, J. L. Gong, X. Chen, A. Kumachev, A. W. Martinez, M. Narovlyansky and G. M. Whitesides, *Lab Chip*, 2010, 10, 477-483.
28. M. Santhiago and L. T. Kubota, *Sensor Actuat B-Chem*, 2013, 177, 224-230.
29. M. Santhiago, J. B. Wydallis, L. T. Kubota and C. S. Henry, *Anal. Chem.*, 2013, 85, 5233-5239.
30. J. L. Delaney, C. F. Hogan, J. F. Tian and W. Shen, *Anal. Chem.*, 2011, 83, 1300-1306.
31. S. M. Wang, L. Ge, X. R. Song, M. Yan, S. G. Ge, J. H. Yu and F. Zeng, *Analyst*, 2012, 137, 3821-3827.
32. H. Wang, N. E. Manicke, Q. A. Yang, L. X. Zheng, R. Y. Shi, R. G. Cooks and O. Y. Zheng, *Anal. Chem.*, 2011, 83, 1197-1201.
33. Q. Yang, H. Wang, J. D. Maas, W. J. Chappell, N. E. Manicke, R. G. Cooks and Z. Ouyang, *Int. J. Mass Spectrom.*, 2012, 312, 201-207.
34. A. K. Yetisen, M. S. Akram and C. R. Lowe, *Lab Chip*, 2013, 13, 2210-2251.
35. E. Evans, E. F. M. Gabriel, W. K. T. Coltro and C. D. Garcia, *Analyst*, 2014, 139, 2127-2132.
36. B. Li, L. Fu, W. Zhang, W. Feng and L. Chen, *Electrophoresis*, 2014, 35, 1152-1159.
37. R. Pelton, *Trends Anal. Chem.*, 2009, 28, 925-942.
38. T. Brooks and C. W. Keevil, *Lett. Appl. Microbiol.*, 1997, 24, 203-206.
39. H. Yagoda, *Ind. Eng. Chem. Anal. Ed.*, **1937**, 9, 79-82.
40. B. Veigas, J. M. Jacob, M. N. Costa, D. S. Santos, M. Viveiros, J. Inacio, R. Martins, P. Barquinha, E. Fortunato and P. V. Baptista, *Lab Chip*, 2012, 12, 4802-4808.
41. R. H. Muller and D. L. Clegg, *Anal. Chem.*, 1949, 21, 1123-1125.
42. A. L. Zhang and Y. Zha, *AIP Adv.*, 2012, 2, 022171, DOI: 10.1063/1061.4733346.
43. Y. Zhang, C. Zhou, J. Nie, S. Le, Q. Qin, F. Liu, Y. Li and J. Li, *Anal. Chem.*, 2014, 86, 2005-2012.
44. A. M. Rosa, A. F. Louro, S. A. Martins, J. Inacio, A. M. Azevedo and D. M. Prazeres, *Anal Chem*, 2014, 86, 4340-4347.
45. T. Nikolic, M. Kostic, J. Praskalo, B. Pejic, Z. Petronijevic and P. Skundric, *Carbohydr. Polym.*, 2010, 82, 976-981.
46. X. Chen, J. Chen, F. Wang, X. Xiang, M. Luo, X. Ji and Z. He, *Biosens. Bioelectron.*, 2012, 35, 363-368.
47. S. A. Bhakta, R. Borba, M. Taba Jr, C. D. Garcia and E. Carrilho, *Anal. Chim. Acta*, 2014, 809, 117-122.
48. S. A. Klasner, A. K. Price, K. W. Hoeman, R. S. Wilson, K. J. Bell and C. T. Culbertson, *Anal. Bioanal. Chem.*, 2010, 397, 1821-1829.
49. M. Kaefer, S. J. Piva, J. A. M. De Carvalho, D. B. Da Silva, A. M. Becker, A. C. Coelho, M. M. M. F. Duarte and R. N. Moresco, *Clin. Biochem.*, 2010, 43, 450-454.
50. P. Schrenkhammer and O. S. Wolfbeis, *Biosens. Bioelectron.*, 2008, 24, 994-999.
51. R. A. McPherson and M. R. Pincus, *Henry`s Clinical Diagnosis and Management by Laboratory Methods*, Saunders, Philadelphia, PA, 22nd. edn., 2011.